ARTICLE
Journal of Cellular Biochemistry 109:1109–1117 (2010)

Journal of Cellular Biochemistry

Protein Kinase C Mediated Intracellular Signaling Pathways Are Involved in the Regulation of Sodium-Dependent Glucose Co-Transporter SGLT1 Activity

Carmen Castaneda-Sceppa,[1] Supriya Subramanian,[2] and Francisco Castaneda[2*]

[1]*Bouve College of Health Sciences, Northeastern University, Boston, Massachusetts*

[2]*Max Planck Institute of Molecular Physiology, Dortmund, Germany*

ABSTRACT

The sodium-dependent glucose co-transporter (SGLT1) is regulated by protein kinases. The aim of the present study was to examine the role of protein kinase C (PKC) in the regulation of rabbit (rb) SGLT1 activity as determined by α-methyl-D-glucopyranoside (AMG) uptake and to identify the cellular mechanisms involved in this process. For this purpose Chinese hamster ovary cells expressing rbSGLT1 (CHO-G6D3) were treated with PKC activators and inhibitors. PKC activators did not exert any effect on AMG uptake, as corroborated by mutation of the putative phosphorylation sites of PKC. In contrast, the PKC inhibitor bisindolylmaleimide I (BIM) increased AMG uptake. This effect was associated with translocation of rbSGLT1 from the intracellular pool to the plasma membrane demonstrated by pre-treatment of G6D3 cells with cytochalasin D that abolished the effect of BIM. In addition, intracellular signaling pathways (p38/MAPK, ERK/MAPK, JNK/MAPK, and PI3K/Akt/mTOR) were associated with PKC-regulated AMG uptake. Moreover, rbSGLT1 mRNA level was higher in BIM-treated cells than in untreated, control cells. This effect was completely abolished by actinomycin D treatment. The present study demonstrates that PKC regulates rbSGLT1 activity via a complex intracellular mechanism that involves sorting and transcriptional regulation of rbSGLT1. The study findings suggest the involvement of two complementary opposite mechanism of action, in which the balance between two antagonistic effects, namely stimulation and inhibition of the transporter, regulates the activity of rbSGLT1 by PKC. J. Cell. Biochem. 109: 1109–1117, 2010.

KEY WORDS: α-METHYL-D-GLUCOPYRANOSIDE UPTAKE; INTRACELLULAR SIGNALING PATHWAYS; PROTEIN KINASE C; SGLT1; TRANSPORTER SORTING

Transepithelial absorption of D-glucose is mediated by secondary active sodium-dependent-D-glucose co-transporter (SGLT) proteins [Hediger and Rhoads, 1994; Wright et al., 2004, 2007]. Different mechanisms have been involved in the regulation of SGLT1 activity based on studies using cell lines expressing SGLT1 as well as cells derived from tissues that constitutively express SGLT1 proteins. In addition to the effect of glucose itself [Dyer et al., 2003a,b, 2007], regulation of SGLT1 activity has been associated with protein kinases. One of the most extensively analyzed effects is that of serine/threonine kinases, including protein kinase A (PKA) and protein kinase C (PKC). The regulatory effect of protein kinases takes place either directly or indirectly [Vayro and Silverman, 1999]. A direct stimulatory effect of protein kinases on membrane transport regulation results in kinetic change of the transporter or carrier turnover number. In contrast, an indirect effect leads to an increased amount of the transporter found in the plasma membrane [Vayro and Silverman, 1999].

Studies using polarized epithelial cell lines [Delezay et al., 1995; Peng and Lever, 1995], *Xenopus* oocytes [Hirsch et al., 1996; Wright et al., 1997], renal epithelial LLC-PK1 cell line derived from porcine kidney proximal tubule cells [Yet et al., 1994], and rat intestinal brush-border membrane vesicles [Ishikawa et al., 1997] have demonstrated an indirect regulatory effect of PKC on rabbit SGLT1 (rbSGLT1). PKC indirectly regulates rbSGLT1 function by increasing the rate at which the protein is localized into the plasma membrane [Wright et al., 1997]. This effect results from increased transporter

Abbreviations: PMA, phorbol-12-myristate-13-acetate; DOG, 1,2-dioctanoyl-*sn*-glycerol; BIM, bisindolylmaleimide I; AACOCF3, arachidonyl trifluoromethyl ketone; PI3K, phosphoinositide-3-kinase; MAPK, mitogen-activated protein kinase.

*Correspondence to: Dr. Francisco Castaneda, Laboratory for Molecular Pathobiochemistry and Clinical Research, Max Planck Institute of Molecular Physiology, Otto-Hahn-Strasse 11, 44227 Dortmund, Germany.
E-mail: francisco.castaneda@mpi-dortmund.mpg.de

Received 6 June 2009; Accepted 7 December 2009 • DOI 10.1002/jcb.22489 • © 2010 Wiley-Liss, Inc.
Published online 12 January 2010 in Wiley InterScience (www.interscience.wiley.com).

trafficking from the intracellular pool to the plasma membrane by endocytosis or exocytosis [Wright et al., 1997]. A similar mechanism has been found in other transporter proteins such as rat brain γ-aminobutyric acid transporter 1 (GAT1) expressed in *Xenopus* oocytes [Corey et al., 1994]. In contrast to the dopamine transporter (DAT1) and the serotonin transporter, this has been shown to be directly regulated by protein kinases [Anderson and Horne, 1992; Kitayama et al., 1994].

PKC is ubiquitously expressed and participates in the regulation of different cellular processes including cell growth and differentiation, endocrine and exocrine secretion, tumor promotion, and cell death [Meinhardt et al., 2000; Basu and Sivaprasad, 2007; Biden et al., 2008]. There are 10 mammalian PKC isozymes classified into four categories (conventional, novel, atypical, and PKC-related kinases) [Newton, 2003]. This classification is based on structural differences in the regulatory domain and different activation conditions [Liu, 1996; Nishikawa et al., 1997]. PKC is regulated by their C1 and C2 domains, which bind diacylglycerol (DAG) [Mellor and Parker, 1998] and Ca^{2+} [Newton, 2003], respectively. In the case of conventional PKCs, regulation is through DAG and Ca^{2+}. In contrast, novel PKCs are regulated by DAG but in a Ca^{2+}-independent manner; these proteins lack a Ca^{2+}-binding C2 domain [Newton, 2003].

PKC activity depends on intracellular molecules known as second messengers including lipids and calcium. PKC requires lipids, such as phospholipase A_2 (PLA_2), phospholipase C (PLC), diacylglycerol (DAG), and phosphatidylinositide-3-kinase (PI3K), to be activated [Toker et al., 1994; Parekh et al., 2000]. Another important second messenger associated with PKC is calcium [Cullen, 2003]. The release of calcium from intracellular stores, induced by inositol triphosphate triggers a phospholipid-dependent translocation of calcium-dependent PKC isoforms to the membrane.

Based on the extended effect of PKC in the regulation of different intracellular processes, the involvement of intracellular signaling pathways induced by PKC in the regulation of rbSGLT1 can be postulated. In the present study, we examined the role of PKC in α-methyl-D-glucopyranoside (AMG) uptake using PKC activators and inhibitors. In addition, the intracellular mechanisms associated with PKC regulation were investigated.

METHODS

DRUGS AND REAGENTS

All chemicals were of the highest purity available from Sigma (Deisenhofen, Germany) unless otherwise indicated. [^{14}C]-AMG (specific radioactivity 300 mCi/mmol) was purchased from Perkin-Elmer (Boston, MA). For immunoblotting, anti-SGLT1 antibody (QIS 30), a glutathione-S-transferase fusion protein containing the extracellular fragment of rabbit SGLT1 (amino acids 243–272, starting with Q, I, S), was used [Kipp et al., 2003].

CELL CULTURE AND TRANSFECTION

Chinese hamster ovary cells stably expressing rbSGLT1 (CHO-G6D3) generated in our laboratory [Lin et al., 1998] were used. We have used these cells as a model to study the intracellular mechanisms of biosynthesis and functional regulation of rbSGLT1 [Raja et al., 2004; Puntheeranurak et al., 2007; Wimmer et al., 2009]. CHO-GD3 cells grown in 25 cm^2 flasks (Falcon, Heidelberg, Germany) under 7.5% CO_2 at 37°C. The cells were cultured to 80% confluence in DMEM (PAN Biotech, Aidenbach, Germany) containing low glucose (5 mM) supplemented with 5% fetal calf serum, 1 mM sodium pyruvate, 2 mM glutamine, 50 μM β-mercaptoethanol, and 400 μg/ml paneticin G420. For transient expression of wild-type rbSGLT1 and T50A, S303A, S418A, and S565A rbSGLT1 mutants, CHO cells grown in 24-well plates (5% CO_2 at 37°C) in DMEM supplemented with 10% fetal calf serum, 2 mM glutamine, and transfected using Superfect Transfection Kit (Qiagen, Hilden, Germany) according to the manufacturer's protocol.

CONSTRUCTION OF MUTANTS IN PUTATIVE PKC PHOSPHORYLATION SITES BY SITE-DIRECTED MUTAGENESIS

Construction of mutants was performed based on the reported four putative PKC serine/threonine phosphorylation sites of rbSGLT1 [Wright et al., 1997] and prepared by site-directed mutagenesis using Quikchange kit (Stratagene, La Jolla, CA). For this purpose the pEGFP C-1 Gateway expression vector containing the specific rbSGLT1 cDNA mutant (T50A, S303A, S418A, or S565A) was used as template and subcloned into pHook-2. Polymerase chain reaction (PCR) was used to generate restriction sites at the ends of insert DNA and digested with *Hin*dIII and *Nhe*I restriction enzymes (NEB, Frankfurt, Germany) followed by ligation to pHook-2. The sequence of mutant cDNA was confirmed by DNA sequencing (Applied Biosystems, Darmstadt, Germany).

[^{14}C] α-METHYL-D-GLUCOPYRANOSIDE (AMG) UPTAKE

Sodium-dependent D-glucose co-transport activity in CHO-G6D3 and CHO (wild-type rbSGLT1 or T50A, S303A, S418A, and S565A rbSGLT1 mutants) cells was determined by measuring the uptake of AMG, a substrate specific for SGLT1. Cells were grown to confluence in 24-well plates at a concentration of 2×10^4 cells/well and maintained in culture for 2 days to allow the cells to form a confluent monolayer [Castaneda and Kinne, 2005]. Prior to the transport assay, the cells were incubated in a D-glucose-free medium for 2 h at 37°C to remove the extracellular D-glucose and to reduce the intracellular glucose concentration [Lin et al., 1998]. For the purpose of this study, Krebs–Ringer–Henseleit (KRH) solution containing 120 mM NaCl, 4.7 mM KCl, 1.2 mM $MgCl_2$, 2.2 mM $CaCl_2$, 10 mM HEPES (pH 7.4 with Tris) was used to assess sodium-dependent D-glucose transport. For sodium-free conditions, KRH solution containing 120 mM *N*-methyl-glucamine (NMG) instead of NaCl (Na^+) was used.

Briefly, cells pre-treated with the indicated drugs for 15 min at 37°C were incubated for 30 min with 500 μl transport buffer containing KRH-Na^+ or KRH-NMG plus [^{14}C]AMG (0.1 μCi/μl). At the end of the uptake period 500 μl of ice-cold stop buffer (KRH-Na^+, containing 0.5 mM phlorizin) was added. Then, cells were solubilized in 2% SDS, the amount of radioactive AMG taken up was counted, and the protein content determined as described by Bradford [1976]. Finally, sodium-dependent uptake was calculated by subtracting the uptake values obtained in the absence of sodium (KRH-NMG) from the values of KRH-sodium and expressed as pmol/mg protein/30 min.

MEMBRANE PREPARATION AND WESTERN BLOT ANALYSIS

CHO-G6D3 cells grown in petri dishes were treated with bisindolylmaleimide I (BIM) (1 μM) for 15 min at 37°C. Then, the cells were scraped from the plates and centrifuged at 500*g* for 10 min at 4°C. The pellet was suspended in 1 ml of ice-cold hypotonic buffer (10 mM HEPES–Tris, 5 mM EGTA-Na^+, and 0.01% thimerosal, pH 7.4) supplemented with protease and phosphatase inhibitors. The cells were lysed by two freeze–thaw cycles and centrifuged at 100,000*g* for 60 min at 4°C to remove the cytosolic proteins. The pellets were solubilized in hypotonic buffer containing 1% Triton X-100 and incubated at 4°C for 30 min. The non-solubilized material was centrifuged again to exclude the non-solubilized material. The supernatants, which represent the membrane protein fraction, were analyzed by Western blotting with the anti-SGLT1 antibody QIS-30 (1:1,000). The quantification of the rbSGLT1 amount was performed by using ImageJ v. 1.34 software for Windows (National Institutes of Health, Bethesda) using the integrated optical density of bands and expressed as fold-values of the average optical density of untreated, control CHO cells. RbSGLT1 signal was corrected relative to β-actin, which was determined using anti-β-actin monoclonal antibody.

IMMUNOCYTOCHEMICAL ANALYSIS

Cells were grown on poly-L-lysine-coated coverslips. After 24 h, the cells were rinsed with PBS and fixed with 3% paraformaldehyde for 20 min. Cells were subsequently permeabilized with 0.1% Triton X-100 for 3 min, and blocked for 20 min with PBG (0.2% gelatin, 0.5% BSA, pH 7.4). Coverslips were then incubated with anti-SGLT1 antibody QIS-30 (1:1,000) in PBS. Cy3-conjugated donkey anti-rabbit IgG antibody (1:500) in PBS + 1% BSA + 3% milk powder for 60 min at room temperature was used as a secondary antibody. Cell nuclei were counterstained with a 4-,6-diamidino-2-phenylindole (DAPI) solution (5 μg/ml). Cellular fluorescent signals were detected using fluorescence microscopy.

QUANTITATIVE REAL-TIME REVERSE TRANSCRIPTION-POLYMERASE CHAIN REACTION (RT-PCR)

Quantitative real-time PCR was used to evaluate the effect of BIM on mRNA rbSGLT1. Total RNA was extracted using RNase kit (Qiagen) and its quality was confirmed by electropherograms using a 2100 BioAnalyzer (Agilent, Santa Clara, CA). Real-time PCR was performed using the QuantiTect SYBR green RT-PCR (reverse transcription-polymerase chain reaction) kit (Qiagen). A quantitative real-time PCR determination using the Optical System Software (iQ5 version 1.0) provided with the BioRad iQ5 cycler (BioRad, Munich, Germany) was performed. Specific primers for rbSGLT1 forward (5′-CAC CAC CAT AAA CAG GCT G-3′) and SGLT1 reverse (5′-AGC CTG ATA GAG CAT TCT TT-3′) were used. All primers were synthesized by MWG Biotech AG (Ebersberg, Germany). Samples were prepared in triplicate and real-time PCR measurement for each sample was done in duplicate. The analysis of relative RT-PCR quantification was calculated using the threshold cycle (CT) method [Pfaffl, 2001]. For normalization, primers for human β-actin forward (5′-GCG CATGGGTCA GAA GGA CT-3′) and β-actin reverse (5′-TCG TCC CAG TTG GTG ACG AT-3′) were used. The average of triplicate real-time PCR measurements was used to calculate the mean induction ratio and standard error (SE).

STATISTICAL ANALYSIS

The data are given as mean and SE from a number (n) of independent experiments. Statistical comparisons between treated versus untreated (control) cells were performed by independent *t*-test analysis. *P*-values less than 0.05 (two tailed) were considered statistically significant.

RESULTS

PROTEIN KINASE C MODULATES rbSGLT1 UPTAKE IN CHO-G6D3 CELLS

As shown in Figure 1, sodium-dependent AMG uptake had mean values of 1,406 ± 34 pmol/mg protein/30 min after phorbol-12-myristate-13-acetate (PMA) treatment (100 nM for 15 min at 37°C) or values of 1,427 ± 42 pmol/mg protein/30 min after 1,2-dioctanoyl-*sn*-glycerol (DOG) treatment (10 μM for 15 min at 37°C). These values were similar to those obtained in the untreated, control cells (n = 24) in which a mean value of 1,493 ± 48 pmol/mg protein/30 min was found. In contrast, treatment with PKC inhibitors (BIM and chelerythrine) resulted in increased sodium-dependent AMG uptake. BIM treatment (1 μM for 15 min at 37°C) resulted in a mean value of 1,906 ± 64 pmol/mg protein/30 min compared to untreated, control cells ($^*P < 0.05$; n = 24). A similar effect was found with chelerythrine treatment (2 μM for 15 min at 37°C) as shown by a mean value of 1,924 ± 59 pmol/mg protein/30 min compared to controls ($^*P < 0.05$; n = 24). These data represent an increase in sodium-dependent AMG uptake equivalent to 28% and 29% after BIM and chelerythrine treatment, respectively.

REMOVAL OF THE PUTATIVE PKC PHOSPHORYLATION SITE OF rbSGLT1 DOES NOT ATTENUATE THE EFFECT OF BIM ON AMG-UPTAKE

To analyze further the effect of PKC on sodium-dependent AMG uptake, point mutations of the putative PKC phosphorylation sites

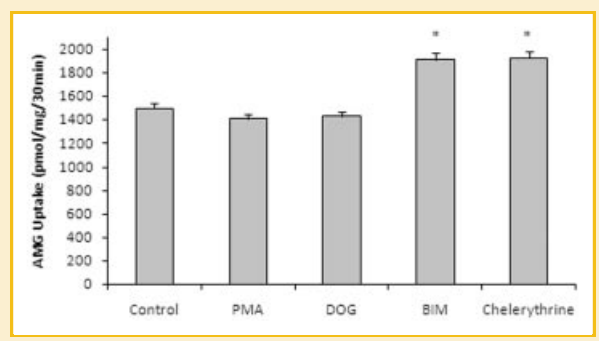

Fig. 1. Effect of PKC activators and inhibitors on sodium-dependent AMG uptake in CHO-G6D3 cells. Cells were pre-incubated at 37°C with PMA (100 nM), DOG (10 μM), BIM (1 μM), or chelerythrine (2 μM) for 15 min prior to uptake experiments and compared to untreated CHO-G6D3 cells (control). The chemical concentration of AMG was 3 μM. AMG uptake was measured after 30 min at 37°C in the presence of the compounds indicated. Results are mean ± SE, n = 24. $^*P < 0.05$ treated versus untreated, control cells.

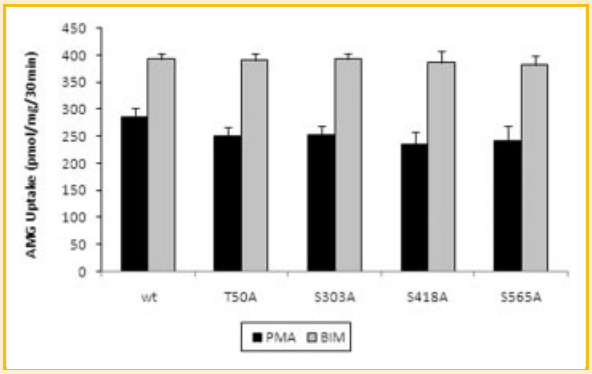

Fig. 2. Effect of mutation of PKC consensus sites on AMG uptake. Wild-type, T50A, S303A, S418A, and S565A rbSGLT1 mutants transiently transfected CHO cells were treated for 15 min with PMA (100 nM) or BIM (1 μM) at 37°C. AMG uptake was measured after 30 min in the presence of the indicated compounds. Values are mean ± SE, n = 24.

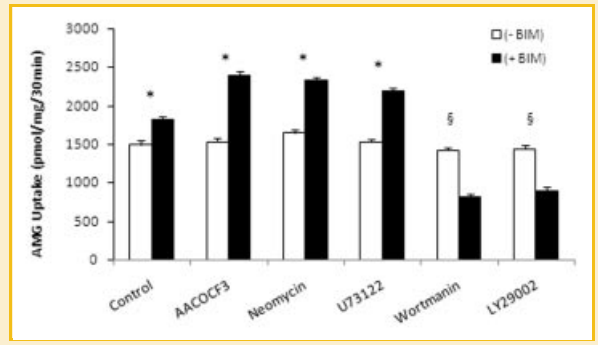

Fig. 3. Effects of PLA_2, PLC, and PI3K inhibitors on BIM-induced PKC-regulated AMG uptake. Cells were pre-incubated with specific inhibitors of PLA_2 (AACOCF3; 10 μM), PLC (neomycin; 100 μM and U73122; 10 μM) or PI3K (wortmanin, 25 nM and LY29002, 1 μM) for 15 min before incubation with BIM (1 μM, +BIM) or without BIM incubation (−BIM). AMG uptake was measured after 30 min at 37°C. Results are mean ± SE, n = 24. $^{*}P < 0.05$ or $^{\S}P < 0.01$ +BIM treated versus −BIM treated, control cells.

(T50A, S303A, S418A, and S565A) of rbSGLT1 was performed. As shown in Figure 2, PMA or BIM treatment did not cause any change in AMG uptake CHO cells transiently transfected with PKC-site mutants (T50A, S303A, S418A, and S565A); as shown by mean values of 250 ± 16 pmol/mg protein/30 min (n = 24) and 379 ± 34 pmol/mg protein/30 min (n = 24) after PMA or BIM treatment, respectively. These values were comparable to those found in wild type, control cells treated with PMA or BIM with values of 285 ± 40 and 392 ± 40 pmol/mg protein/30 min, respectively.

INVOLVEMENT OF SECOND MESSENGERS IN PKC-REGULATED AMG UPTAKE

To analyze further the mechanism of action of PKC on AMG uptake, the effect of specific inhibitors of second messenger molecules, including PLA_2, PLC, and PI3K were analyzed. For this purpose, CHO-G6D3 cells were pre-treated with the specific inhibitors for 15 min and subsequently exposed to PKC inhibitor (1 μM BIM for 15 min, +BIM) and compared to cells not exposed to BIM (−BIM). As shown in Figure 3, +BIM control cells significantly increased AMG uptake (1,816 ± 45 pmol/mg protein/30 min vs. −BIM control cells, 1,491 ± 56 pmol/mg protein/30 min, $^{*}P < 0.05$; n = 24). AMG uptake was also significantly increased in CHO-G6D3 cells pre-treated with the PLA_2 inhibitor AACOCF3 (+BIM 2,388 ± 47 pmol/mg protein/30 min; $^{*}P < 0.05$; n = 24) compared to −BIM AACOCF3 pre-treated cells (1,525 ± 39 pmol/mg protein/30 min). Similar effects were observed with PLC inhibitors (+BIM neomycin and U73122 pre-treated cells), which showed mean values of 2,325 ± 35 and 2,188 ± 40 pmol/mg protein/30 min, respectively, compared to the value obtained with −BIM neomycin and U73122 in which values of 1,643 ± 45 and 1,529 ± 30 pmol/mg protein/30 min, respectively, were shown ($^{*}P < 0.05$; n = 24). These effects represented a 57%, 41%, and 43% increase in AMG uptake induced by BIM after pre-treatment with AACOCF3, neomycin, and U73122 inhibitors, respectively.

In contrast, pre-treatment with PI3K inhibitors wortmanin (25 nM) and LY29002 (1 μM) abolished the effect of BIM on AMG uptake as shown by a significant reduction in AMG uptake values of 810 ± 35 and 889 ± 47 pmol/mg protein/30 min ($^{\S}P < 0.001$; n = 24) in +BIM pre-treated cells with wortmanin and LY29002, respectively. These values were significantly lower than those found in CHO-G6D3 control cells exposed to BIM in which a value of 1,816 ± 45 pmol/mg protein/30 min was found. Moreover, the effect of both inhibitors in −BIM cells pre-treated with wortmanin and LY29002, demonstrated AMG uptake values of 1,420 ± 36 and 1,435 ± 3 pmol/mg protein/30 min, respectively ($^{\S}P < 0.01$; n = 24). These values were comparable to those found in −BIM untreated, control cells which showed values of 1,491 ± 56 pmol/mg protein/30 min. These findings demonstrate a direct involvement of PI3K on BIM-induced stimulation of rbSGLT1 and suggest a subsequent activation of intracellular signaling pathways.

INVOLVEMENT OF INTRACELLULAR SIGNALING PATHWAYS IN PKC-REGULATED AMG UPTAKE

To determine the involvement of intracellular signaling pathways in PKC-regulated AMG uptake, CHO-G6D3 cells were incubated with the following inhibitors: SB203580 (a p38 mitogen-activated protein kinase (MAPK) inhibitor; 1 μM), PD98059 (an ERK/MAPK inhibitor; 10 μM), SP600125 (a Jun kinase inhibitor; 1 μM), KP372-1 (an Akt inhibitor; 10 μM), and rapamycin (a mTOR inhibitor; 25 nM) for 15 min each and compared to cells treated with BIM alone without pre-treatment with any of the respective inhibitors (referred to as no pre-tx or control cells). As shown in Figure 4A, pre-treatment with SB203580 resulted in a 24% increase in SGLTl activity, as demonstrated by AMG uptake of 2,344 ± 51 pmol/mg protein/30 min compared to no pre-tx cells, in which a value of 1,890 ± 39 pmol/mg protein/30 min was observed ($^{*}P < 0.05$; n = 24). In contrast, PD98059 and SP600125 resulted in significant reductions in AMG uptake of 22% and 25%, respectively, compared with no-pre-tx cells ($^{*}P < 0.05$; n = 24). Pre-treatment with PD98059 and SP600125 completely abolished the effect of BIM on AMG uptake, as demonstrated by values of 1,419 ± 41 or 1,417 ± 32 pmol/mg protein/30 min, respectively. These values are similar to those found

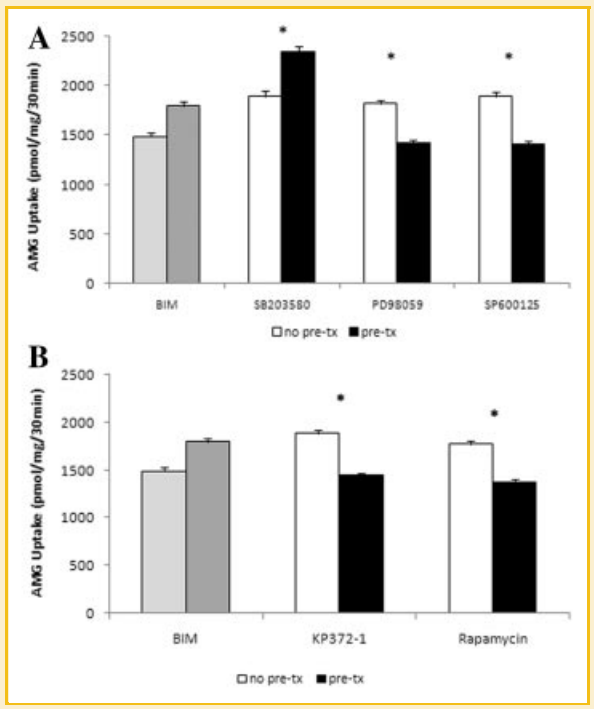

Fig. 4. Involvement of intracellular signaling pathways in BIM-induced PKC-regulated AMG uptake. A: Cells were pre-incubated with specific inhibitors for MAPK; SB203580 (p38 MAPK; 1 μM), PD98059 (MEK/MAPK; 10 μM), and SP600125 (JNK; 1 μM), or B: specific inhibitors for Akt (KP372-1; 10 μM) and mTOR (rapamycin; 25 nM) for 15 min before incubation with BIM (1 μM) and compared to cells treated with BIM alone without pre-treatment exposure to any of the respective inhibitors. AMG uptake was measured after 30 min at 37°C. Results are mean ± SE, n = 24. $^{*}P < 0.05$ treated (pre-tx) versus untreated, control cells (no pre-tx).

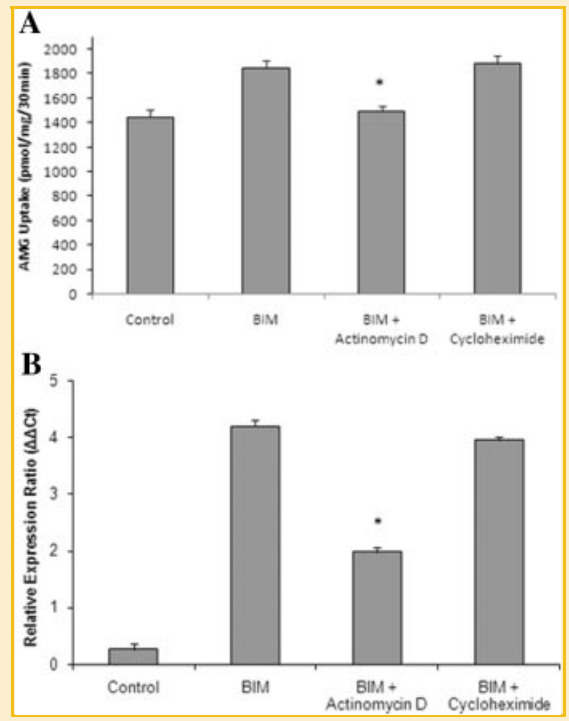

Fig. 5. Effect of actinomycin D and cycloheximide on BIM-induced PKC-regulated AMG uptake. A: AMG uptake in CHO-G6D3 BIM-treated cells after pre-treatment with actinomycin D (0.1 μM) or cycloheximide (1 μM) for 15 min. AMG uptake determination was performed 6 h later. B: Median relative expression ratios ($2^{\Delta\Delta Ct}$) for rbSGLT1 mRNA levels in CHO-G6D3 cells after pre-treatment with actinomycin D or cycloheximide. Results are mean ± SE, n = 16. $^{*}P < 0.01$ BIM-treated versus BIM-untreated cells.

in cells without BIM treatment (as shown in Fig. 1) and corroborate the involvement of MAPK pathway in PKC regulation of rbSGLT1 mediated by the ERK/MAPK and JNK pathways.

To examine the role of the Akt pathway in PKC-regulated increase in AMG uptake, CHO-G6D3 cells were pre-treated with KP372-1 (an Akt inhibitor; 10 μM) for 30 min before BIM treatment. Figure 4B shows that there is a role for the Akt pathway in the regulation of rbSGLT1 in CHO-G6D3 cells as demonstrated by a reduction of BIM-induced AMG uptake (1,444 ± 28 pmol/mg protein/30 min) in pre-treated cells with KP372-1 (10 μM). Specifically, the Akt inhibitor significantly blocked the BIM-induced increase in AMG uptake ($^{*}P < 0.05$; n = 24). The same effect was observed when rapamycin, an mTOR inhibitor (25 nM), was used. Pre-treatment with rapamycin resulted in an AMG uptake value of 1,370 ± 36 pmol/mg protein/30 min compared to no pre-tx cells without pre-treatment with rapamycin ($^{*}P < 0.05$; n = 24). These data corroborates the involvement of Akt/mTOR pathway in PKC-regulated AMG uptake.

EFFECT OF ACTINOMYCIN D AND CYCLOHEXIMIDE ON PKC-REGULATED AMG UPTAKE

To evaluate the effect of PKC on transcriptional and translational regulation of rbSGLT1, pre-treatment with specific inhibitors for 15 min with subsequent determination of AMG uptake and mRNA levels 6 h later were performed. As shown in Figure 5A, pre-treatment of CHO-G6D3 cells with actinomycin D (0.1 μM for 15 min) abolished the effect of BIM on AMG uptake as shown by AMG uptake values of 1,495 ± 42 pmol/mg protein/30 min compared to 1,848 ± 58 pmol/mg protein/30 min found in BIM cells without actinomycin D ($^{*}P < 0.01$; n = 16). On the other hand, cycloheximide (1 μM for 15 min) did not cause any effect on BIM-induced AMG uptake as demonstrated by similar values in pre-treated and BIM-treated cells without cycloheximide pre-treatment (1,883 ± 64 and 1,848 ± 58 pmol/mg protein/30 min, respectively). To analyze further the effect of PKC-regulated AMG uptake, rbSGLT1 mRNA amount was determined (Fig. 5B). Actinomycin D treated cells had an rbSGLT1 mRNA ratio of 1.98 as compared to BIM-treated cells without actinomycin D in which a ratio of 4.2 was found. This represents a 2.2-fold reduction as compared to BIM-treated cells ($^{*}P < 0.01$; n = 16). Cycloheximide-treated cells showed a slight but non-significant decrease in SGLT1 mRNA as shown by a ratio of 3.95, which is similar to that found in BIM-treated cells without cycloheximide. The amount of rbSGLT1 mRNA found in untreated, control cells demonstrated a ratio of 0.3 which is significantly lower than those found in BIM-treated cells. This data corroborate the induction of SGLT1 mRNA by BIM as well as a transcriptional regulation.

PKC INHIBITION INCREASES THE INSERTION OF rbSGLT1 INTO THE PLASMA MEMBRANE

The effect of PKC inhibition on rbSGLT1 expression in membrane protein fraction is shown in Figure 6. Figure 6A shows representative microscopic images of the immunostaining analysis. G6D3 cells treated with BIM (1 μM) caused a slight increase in the distribution of SGLT1 labeled with the anti-SGLT1 antibody (QIS-30) as compared to untreated, control cells. To be able to quantify this effect Western blot analysis of the cell membrane fraction was performed (Fig. 6B). The amount of rbSGLT1 blotted from plasma membrane fraction in CHO-G6D3 cells treated with BIM corrected to β-actin was higher than that in untreated, control cells ($^{*}P < 0.05$; n = 6), as shown by an integrated density of 4.2 ± 0.3 and 2.2 ± 0.4 arbitrary units, respectively.

To further evaluate the effect of PKC on the insertion of rbSGLT1 into the plasma membrane through membrane trafficking, the effect of cytochalasin D, an actin filament disruptor, was determined. As shown in Figure 6C, in the absence of cytochalasin D, BIM stimulates the transport activity of CHO-G6D3 cells to 1,848 ± 58 pmol/mg protein/30 min as compared to untreated, control cells (1,448 ± 47 pmol/mg protein/30 min, $^{*}P < 0.01$; n = 24). This result represents an increase in sodium-dependent AMG uptake equivalent to 28%. In contrast, in pre-treated cytochalasin D cells the effect of BIM was abolished, as shown by uptake values of 1,396 ± 36 pmol/mg protein/30 min compared to BIM-treated cells ($^{\S}P < 0.01$; n = 24). These data corroborate the translocation and insertion of rbSGLT1 into the plasma membrane in BIM-treated cells.

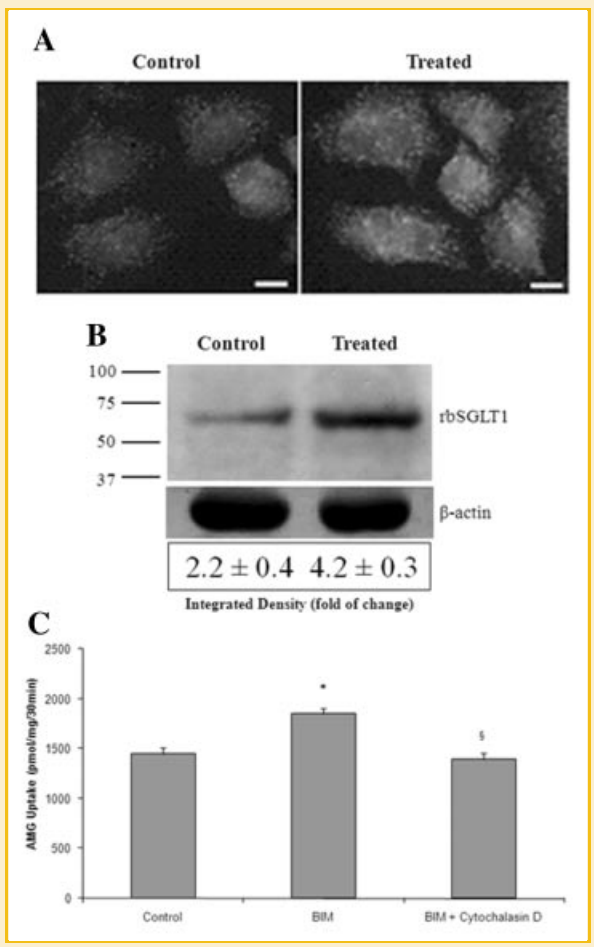

Fig. 6. Effect of BIM on the insertion of SGLT1 into the plasma membrane. A: Representative immunostaining images for rbSGLT1 in CHO-G6D3 cells treated with BIM (1 μM for 15 min at 37°C) compared to untreated, control cells. B: Plasma membrane fractions from both treated and untreated, control cells (20 μg protein/lane) blotted with an anti-SGLT1 antibody (QIS-30; 1:1,000) with quantitative analysis of the blotted rbSGLT1, corrected to β-actin, using the integrated optical density of bands, and expressed as arbitrary units of the average optical density of CHO cells. Values are mean ± SE, n = 6. $^{*}P < 0.05$ treated versus untreated, control cells. C: Effect of cytochalasin D on BIM-induced AMG uptake in CHO-G6D3 cells. Results are mean ± SE, n = 24. $^{*}P < 0.01$ treated versus untreated, control cells or $^{\S}P < 0.01$ cytochalasin D treated versus untreated, control cells.

DISCUSSION

The effect of PKC activators (such as PMA and DOG) on rbSGLT1 is characterized by an isoform-dependent response. While PKC activation decreases sugar uptake by rabbit and rat SGLT1, the same activators increases transport by human SGLT1 [Hirsch et al., 1996]. Interestingly, studies performed in different cell culture systems demonstrated a different degree on the effect of PKC activators on sugar uptake. Studies performed in oocytes expressing rabbit SGLT1 have demonstrated a decrease of 60% [Wright et al., 1997], while studies performed in COS7 cells showed a decrease of about 38%. These variations depend on the amount of rbSGLT1 expressed in each cell type. Our data corroborate the reported effect of PKC activators on rbSGLT1, namely a reduction in AMG uptake in rbSGLT1. We found a reduction of 6% in CHO-G6D3 cells expressing rbSGLT1. The slight reduction in the AMG uptake we found can be explained by the different amount of rbSGLT1 expressed in the different cell culture system used. In oocytes injected with rbSGLT1 cRNA a 500–1,000 times greater rate of sodium-dependent glucose transport than in non-injected oocytes has been reported [Wright et al., 1997], while in CHO-G6D3 cells a 50-fold higher content of rbSGLT1 can be deduced from the labeling experiments and the protein determinations [Lin et al., 1998].

Studies performed in oocytes expressing rbSGLT1 demonstrated that PKC inhibition directly regulates the activity of rbSGLT1 by increasing the turnover rate of the protein [Vayro and Silverman, 1999]. The data obtained in the present study, however, suggests that the regulation of PKC on rbSGLT1 activity is not only due to a direct phosphorylation of the carrier. This assumption was corroborated by the fact that mutation of the putative phosphorylation sites of PKC did not cause any effect on sodium-dependent AMG uptake in CHO cells transiently expressing rbSGLT1 treated with PKC activators or PKC inhibitors, such as PMA or BIM, respectively. In addition, it suggests the involvement of an indirect regulatory mechanism of action mediated by PKC. The indirect effect of PKC on rbSGLT1 has been associated with the number of the carried found in the plasma membrane. Such mechanism involves rbSGLT1 trafficking from the intracellular pool to the plasma membrane taking place through regulation of exocytosis and

endocytosis [Wright et al., 1997; Vayro et al., 1998]. Our data confirm that a BIM-induced effect depends on translocation and insertion of rbSGLT1 into the plasma membrane. This finding was demonstrated by pre-treatment with cytochalasin D, an actin filament disruptor that abolished the effect of BIM on PKC-regulated AMG uptake. The effect of PKC on rbSGLT1 trafficking seems to be similar to that reported by PKA [Subramanian et al., 2009], suggesting a possible complementary effect of these two protein kinases on the regulation of rbSGLT1. Interestingly, unlike PKA, PKC does not have a direct effect on rbSGLT1. PKA phosphorylation induces conformational changes which alter the functional properties of the transporter [Subramanian et al., 2009].

Due to the complexity of the indirect effect of PKC on rbSGLT1, we postulated that such complementary mechanism involves the participation of intracellular signaling pathways. In contrast to other transporters, such as the Na^+/H^+ exchanger expressed in fibroblast cells [Yip et al., 1997] as well as human SGLT1 [Vayro and Silverman, 1999] that are regulated by PKC activators, activation of PKC by phorbol ester in rbSGLT1 results in a decrease in transporter activity [Vayro and Silverman, 1999]. Our data corroborate this effect. A possible explanation for this difference might be the involvement of different PKC isoenzymes that differs between species [Nishizuka, 1986; Stabel and Parker, 1991; Liu, 1996]. Another possible mechanism responsible for this difference might be the activation of second messenger molecules that are specific for each PKC isoenzyme. We found the involvement of second messenger molecules, namely PLA_2, PLC, and PI3K, in the regulation of AMG uptake by PKC. This effect was demonstrated by pre-treatment with inhibitors of second messenger molecules.

The most strikingly and novel finding obtained in the present study was that regulation of rbSGLT1 by PKC involves the participation of intracellular signaling pathways triggered through second messengers. The regulation of AMG uptake induced by PKC was mediated by at least two distinct intracellular signal cascades involving, on one hand, MAPK (p38/MAPK, MEK/MAPK, and JNK pathways) and on the other PI3K/Akt/mTOR signaling. These findings provide an important insight into the molecular mechanism of action exerted by PKC in the regulation of rbSGLT1.

The involvement of MAPK in PKC-regulated AMG uptake we found corroborates the reported involvement of MAPK signaling in rbSGLT1 in primary cultured rabbit renal proximal tubule cells. In these cells, both epinephrine [Kim et al., 2004] and angiotensin II [Han et al., 2004] inhibited AMG uptake in a time- and dose-dependent manner associated with PKC. Interestingly, studies performed in Sprague–Dawley rats suggested that high glucose concentrations induce cellular hypertrophy and transforming growth factor β expression in renal tubular cells [Fujita et al., 2004]. Such regulation depends on phosphorylation of PLA_2 by MAPK. It has been reported that MAPK phosphorylates cytosolic PLA_2 at Ser-505 [Lin et al., 1993]. This site is identical to the site of cPLA2 phosphorylation induced by phorbol ester. Replacement of Ser-505 with Ala resulted in a PLA_2 mutant that is not a substrate for MAPK [Lin et al., 1993].

The other intracellular signaling pathway involved in the regulation of rbSGLT1 by PKC was the PI3K/Akt/mTOR. Our data demonstrated that PI3K/Akt/mTOR increases the activity of rbSGLT1. It has been reported that PI3K-dependent signaling pathway stimulated by PKC βII regulate the expression of GLUT2 [Helliwell et al., 2003]. Such effect has been controlled by phosphorylation at three different sites of PKC, localized at Thr-500, Thr-641, and Ser-660 [Newton, 1997; Parekh et al., 2000]. Phosphorylation of Thr-500 leads to autophosphorylation of Thr-641 and Ser-660 [Behn-Krappa and Newton, 1999]. Phosphorylation at all three sites are required for activation of PKC βII. Additionally, the data of the present study correlate with the reported involvement of PI3K in the regulation of SGLT1 transport activity in rat jejunum induced by glucagon-like peptide 2 [Cheeseman, 1997]. PI3K activated by glucagon-like peptide 2 was shown to induce the translocation of SGLT1 from the intracellular compartment to the plasma membrane [Cheeseman, 1997]. In addition, PI3K has also been found to be involved in the regulation of other transporters, including sodium-dependent taurocholate co-transport [Webster and Anwer, 1999] and sodium-dependent phosphate transport [Zhen et al., 1997].

Interestingly, we observed that PKC was involved in two opposite mechanisms of action. The first one was an increase in AMG uptake mediated by both MAPK (ERK/MAPK and JNK/MAPK) as well as PI3K/Akt/mTOR signaling pathways, as demonstrated by the blockage of AMG uptake with specific inhibitors. The second mechanism of action was a decrease in AMG uptake mediated by p38/MAPK signaling pathway. The involvement of these two complementary mechanisms of action in the regulation of rbSGLT1 by PKC suggests a balance between two antagonistic effects, namely stimulation and inhibition of the transporter. This finding suggests that PKC has the ability to shift the balance as needed toward stimulation or inhibition. A similar balance response between two opposite effects has been reported with apoptosis where the balance between apoptotic and anti-apoptotic pathways has been observed based on physiologic state [Nair et al., 2004; Castaneda and Rosin-Steiner, 2006].

Another important finding of the present study is the increased expression of rbSGLT1 mRNA induced by BIM. This finding correlates with the reported reduction of rbSGLT1 protein level induced by epinephrine [Kim et al., 2004]. In addition, studies using LLC-PK1 cells have demonstrated that PKC activation decreased SGLT1 mRNA due to mRNA degradation [Shioda et al., 1994]. Degradation of mRNA due to PKC activation has also been shown in thymocytes in which CD4 mRNA degradation has been reported [Takahama and Singer, 1992]. This finding suggests that PKC inhibitors, such as BIM, could induce an opposite effect, namely the increased expression of SGLT1. This assumption seems to be confirmed by the effect of actinomycin D we observed. Actinomycin D decreased BIM-induced SGLT1 mRNA level suggesting the existence of a mechanism by which PKC regulates the amount of mRNA not by direct phosphorylation of PKC or phosphorylation of effector molecules (such as ribonucleases). Moreover, it suggests a transcriptional regulation of rbSGLT1 mRNA induced by BIM. A similar effect has been reported with GLUT2 and GLUT5 mRNA [Jiang and Ferraris, 2001; Cui et al., 2003]. Transcriptional regulation of GLUT5 mRNA expression has been confirmed by increased expression of transcription factors such as fos and jun [Jiang and Ferraris, 2001].

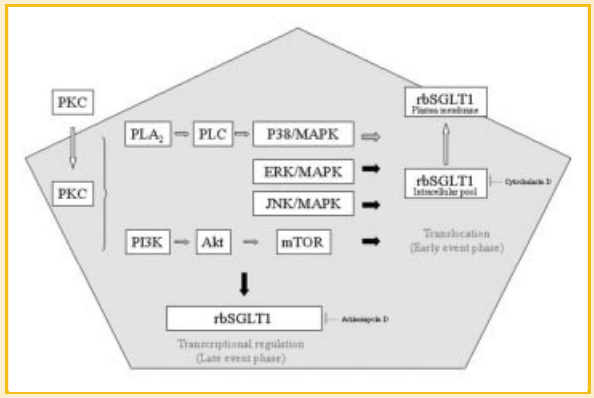

Fig. 7. Proposed regulatory mechanism of PKC in CHO-G6D3 cells resulting from sorting and protein expression of rbSGLT1 mediated by intracellular signaling pathways. The effect of PKC on rbSGLT1 activity was divided into an early- and late-event phases. Black and gray arrows represent stimulation and inhibition of rbSGLT1 activity, respectively.

Taking these data together, we propose a regulatory mechanism of action of PKC on rbSGLT1 that affects sorting and protein expression of rbSGLT1. Figure 7 summarizes the proposed regulation of rbSGLT1 through PKC in CHO-G6D3 cells. Specifically, PKC inhibition induced a biphasic effect on rbSGLT1 regulation, characterized by a rapid transient effect on rbSGLT1 translocation, after 15 min exposure, followed by a rapid AMG uptake due to an increased translocation and insertion of rbSGLT1 into the plasma membrane (early-event phase), and a second persistent activation of gene expression that began after 6 h (late-event phase). The late-event phase is triggered by second messenger molecules (PLA_2, PLC, and PI3K) with subsequent activation of intracellular signaling pathways (MAPK and PI3K/Akt/mTOR).

In conclusion, the present study demonstrates that PKC regulates rbSGLT1-mediated AMG uptake. This effect is due to an indirect effect of PKC on rbSGLT1. This effect concerns a change in the sorting of the transporter between intracellular compartments and the plasma membrane, which results in an increased number of transporters in the plasma membrane. In addition, activation of intracellular signaling pathways triggered by second messenger molecules with subsequent transcriptional regulation of rbSGLT1 mRNA expression. This new information points to an important complementary mechanism in the regulation of SGLT1-mediated glucose transporter in epithelial cells which should be investigated further.

ACKNOWLEDGMENTS

We thank Dr. Rolf Kinne for his valuable support and Petra Glitz for the excellent technical assistance. We also acknowledge the financial support of the International Max Planck Research School in Chemical Biology, Dortmund, Germany.

REFERENCES

Anderson GM, Horne WC. 1992. Activators of protein kinase C decrease serotonin transport in human platelets. Biochim Biophys Acta 1137:331–337.

Basu A, Sivaprasad U. 2007. Protein kinase C epsilon makes the life and death decision. Cell Signal 19:1633–1642.

Behn-Krappa A, Newton AC. 1999. The hydrophobic phosphorylation motif of conventional protein kinase C is regulated by autophosphorylation. Curr Biol 9:728–737.

Biden TJ, Schmitz-Peiffer C, Burchfield JG, Gurisik E, Cantley J, Mitchell CJ, Carpenter L. 2008. The diverse roles of protein kinase C in pancreatic beta-cell function. Biochem Soc Trans 36:916–919.

Bradford MM. 1976. A rapid and sensitive method for the quantitation of microgram quantities of protein utilizing the principle of protein-dye binding. Anal Biochem 72:248–254.

Castaneda F, Kinne RKH. 2005. A 96-well automated method to study inhibitors of human sodium-dependent D-glucose transport. Mol Cell Biochem 280:91–98.

Castaneda F, Rosin-Steiner S. 2006. Low concentration of ethanol induce apoptosis in HepG2 cells: Role of various signal transduction pathways. Int J Med Sci 3:160–167.

Cheeseman CI. 1997. Upregulation of SGLT-1 transport activity in rat jejunum induced by GLP-2 infusion in vivo. Am J Physiol 273:R1965–R1971.

Corey JL, Davidson N, Lester HA, Brecha N, Quick MW. 1994. Protein kinase C modulates the activity of a cloned gamma-aminobutyric acid transporter expressed in Xenopus oocytes via regulated subcellular redistribution of the transporter. J Biol Chem 269:14759–14767.

Cui XL, Jiang L, Ferraris RP. 2003. Regulation of rat intestinal GLUT2 mRNA abundance by luminal and systemic factors. Biochim Biophys Acta 1612: 178–185.

Cullen PJ. 2003. Calcium signalling: The ups and downs of protein kinase C. Curr Biol 13:R699–R701.

Delezay O, Baghdiguian S, Fantini J. 1995. The development of Na(+)-dependent glucose transport during differentiation of an intestinal epithelial cell clone is regulated by protein kinase C. J Biol Chem 270:12536–12541.

Dyer J, Vayro S, King TP, Shirazi-Beechey SP. 2003a. Glucose sensing in the intestinal epithelium. Eur J Biochem 270:3377–3388.

Dyer J, Vayro S, Shirazi-Beechey SP. 2003b. Mechanism of glucose sensing in the small intestine. Biochem Soc Trans 31:1140–1142.

Dyer J, Daly K, Salmon KS, Arora DK, Kokrashvili Z, Margolskee RF, Shirazi-Beechey SP. 2007. Intestinal glucose sensing and regulation of intestinal glucose absorption. Biochem Soc Trans 35:1191–1194.

Fujita H, Omori S, Ishikura K, Hida M, Awazu M. 2004. ERK and p38 mediate high-glucose-induced hypertrophy and TGF-beta expression in renal tubular cells. Am J Physiol Renal Physiol 286:F120–F126.

Han HJ, Park SH, Lee YJ. 2004. Signaling cascade of ANG II-induced inhibition of alpha-MG uptake in renal proximal tubule cells. Am J Physiol Renal Physiol 286:F634–F642.

Hediger MA, Rhoads DB. 1994. Molecular physiology of sodium-glucose cotransporters. Physiol Rev 74:993–1026.

Helliwell PA, Rumsby MG, Kellett GL. 2003. Intestinal sugar absorption is regulated by phosphorylation and turnover of protein kinase C betaII mediated by phosphatidylinositol 3-kinase- and mammalian target of rapamycin-dependent pathways. J Biol Chem 278:28644–28650.

Hirsch JR, Loo DD, Wright EM. 1996. Regulation of Na+/glucose cotransporter expression by protein kinases in *Xenopus laevis* oocytes. J Biol Chem 271:14740–14746.

Ishikawa Y, Eguchi T, Ishida H. 1997. Mechanism of beta-adrenergic agonist-induced transmural transport of glucose in rat small intestine. Regulation of phosphorylation of SGLT1 controls the function. Biochim Biophys Acta 1357:306–318.

Jiang L, Ferraris RP. 2001. Developmental reprogramming of rat GLUT-5 requires de novo mRNA and protein synthesis. Am J Physiol Gastrointest Liver Physiol 280:G113–G120.

Kim EJ, Lee YJ, Lee JH, Han HJ. 2004. Effect of epinephrine on alpha-methyl-D-glucopyranoside uptake in renal proximal tubule cells. Cell Physiol Biochem 14:395–406.

Kipp H, Khoursandi S, Scharlau D, Kinne RK. 2003. More than apical: Distribution of SGLT1 in Caco-2 cells. Am J Physiol Cell Physiol 285: C737–C749.

Kitayama S, Dohi T, Uhl GR. 1994. Phorbol esters alter functions of the expressed dopamine transporter. Eur J Pharmacol 268:115–119.

Lin LL, Wartmann M, Lin AY, Knopf JL, Seth A, Davis RJ. 1993. cPLA2 is phosphorylated and activated by MAP kinase. Cell 72:269–278.

Lin JT, Kormanec J, Wehner F, Wielert-Badt S, Kinne RK. 1998. High-level expression of Na+/D-glucose cotransporter (SGLT1) in a stably transfected Chinese hamster ovary cell line. Biochim Biophys Acta 1373:309–320.

Liu JP. 1996. Protein kinase C and its substrates. Mol Cell Endocrinol 116: 1–29.

Meinhardt G, Roth J, Totok G. 2000. Protein kinase C activation modulates pro- and anti-apoptotic signaling pathways. Eur J Cell Biol 79:824–833.

Mellor H, Parker PJ. 1998. The extended protein kinase C superfamily. Biochem J 332(Pt 2): 281–292.

Nair VD, Yuen T, Olanow CW, Sealfon SC. 2004. Early single cell bifurcation of pro- and antiapoptotic states during oxidative stress. J Biol Chem 279: 27494–27501.

Newton AC. 1997. Regulation of protein kinase C. Curr Opin Cell Biol 9:161–167.

Newton AC. 2003. Regulation of the ABC kinases by phosphorylation: Protein kinase C as a paradigm. Biochem J 370:361–371.

Nishikawa K, Toker A, Johannes FJ, Songyang Z, Cantley LC. 1997. Determination of the specific substrate sequence motifs of protein kinase C isozymes. J Biol Chem 272:952–960.

Nishizuka Y. 1986. Studies and perspectives of protein kinase C. Science 233:305–312.

Parekh DB, Ziegler W, Parker PJ. 2000. Multiple pathways control protein kinase C phosphorylation. EMBO J 19:496–503.

Peng H, Lever JE. 1995. Post-transcriptional regulation of Na+/glucose cotransporter (SGTL1) gene expression in LLC-PK1 cells. Increased message stability after cyclic AMP elevation or differentiation inducer treatment. J Biol Chem 270:20536–20542.

Pfaffl MW. 2001. A new mathematical model for relative quantification in real-time RT-PCR. Nucleic Acids Res 29:e45.

Puntheeranurak T, Wimmer B, Castaneda F, Gruber HJ, Hinterdorfer P, Kinne RK. 2007. Substrate specificity of sugar transport by rabbit SGLT1: Single-molecule atomic force microscopy versus transport studies. Biochemistry 46:2797–2804.

Raja MM, Kipp H, Kinne RK. 2004. C-terminus loop 13 of Na+ glucose cotransporter SGLT1 contains a binding site for alkyl glucosides. Biochemistry 43:10944–10951.

Shioda T, Ohta T, Isselbacher KJ, Rhoads DB. 1994. Differentiation-dependent expression of the Na+/glucose cotransporter (SGLT1) in LLC-PK1 cells: Role of protein kinase C activation and ongoing transcription. Proc Natl Acad Sci USA 91:11919–11923.

Stabel S, Parker PJ. 1991. Protein kinase C. Pharmacol Ther 51:71–95.

Subramanian S, Glitz P, Kipp H, Kinne RK, Castaneda F. 2009. Protein kinase-A affects sorting and conformation of the sodium-dependent glucose co-transporter SGLT1. J Cell Biochem 106:444–452.

Takahama Y, Singer A. 1992. Post-transcriptional regulation of early T cell development by T cell receptor signals. Science 258:1456–1462.

Toker A, Meyer M, Reddy KK, Falck JR, Aneja R, Aneja S, Parra A, Burns DJ, Ballas LM, Cantley LC. 1994. Activation of protein kinase C family members by the novel polyphosphoinositides PtdIns-3,4-P2 and PtdIns-3,4,5-P3. J Biol Chem 269:32358–32367.

Vayro S, Silverman M. 1999. PKC regulates turnover rate of rabbit intestinal Na+-glucose transporter expressed in COS-7 cells. Am J Physiol 276:C1053–C1060.

Vayro S, Lo B, Silverman M. 1998. Functional studies of the rabbit intestinal Na+/glucose carrier (SGLT1) expressed in COS-7 cells: Evaluation of the mutant A166C indicates this region is important for Na+-activation of the carrier. Biochem J 332(Pt 1): 119–125.

Webster CR, Anwer MS. 1999. Role of the PI3K/PKB signaling pathway in cAMP-mediated translocation of rat liver Ntcp. Am J Physiol 277:G1165–G1172.

Wimmer B, Raja M, Hinterdorfer P, Gruber H, Kinne R. 2009. C-terminal loop 13 of Na+/glucose cotransporter 1 contains both stereospecific and non-stereospecific sugar interaction sites. J Biol Chem 284:983–991.

Wright EM, Hirsch JR, Loo DD, Zampighi GA. 1997. Regulation of Na+/glucose cotransporters. J Exp Biol 200:287–293.

Wright EM, Loo DD, Hirayama BA, Turk E. 2004. Surprising versatility of Na+-glucose cotransporters: SLC5. Physiology (Bethesda) 19:370–376.

Wright EM, Hirayama BA, Loo DF. 2007. Active sugar transport in health and disease. J Intern Med 261:32–43.

Yet SF, Kong CT, Peng H, Lever JE. 1994. Regulation of Na+/glucose cotransporter (SGLT1) mRNA in LLC-PK1 cells. J Cell Physiol 158:506–512.

Yip JW, Ko WH, Viberti G, Huganir RL, Donowitz M, Tse CM. 1997. Regulation of the epithelial brush border Na+/H+ exchanger isoform 3 stably expressed in fibroblasts by fibroblast growth factor and phorbol esters is not through changes in phosphorylation of the exchanger. J Biol Chem 272:18473–18480.

Zhen X, Bonjour JP, Caverzasio J. 1997. Platelet-derived growth factor stimulates sodium-dependent Pi transport in osteoblastic cells via phospholipase C gamma and phosphatidylinositol 3′-kinase. J Bone Miner Res 12: 36–44.